Search for High Mass Photon Pairs in $p\overline{p} \rightarrow \gamma\gamma jj$ Events at $\sqrt{s} = 1.8$ TeV

B. Abbott,[30] M. Abolins,[27] B.S. Acharya,[45] I. Adam,[12] D.L. Adams,[39] M. Adams,[17] S. Ahn,[14] H. Aihara,[23] G.A. Alves,[10] N. Amos,[26] E.W. Anderson,[19] R. Astur,[44] M.M. Baarmand,[44] A. Baden,[25] V. Balamurali,[34] J. Balderston,[16] B. Baldin,[14] S. Banerjee,[45] J. Bantly,[5] E. Barberis,[23] J.F. Bartlett,[14] K. Bazizi,[41] A. Belyaev,[28] S.B. Beri,[36] I. Bertram,[33] V.A. Bezzubov,[37] P.C. Bhat,[14] V. Bhatnagar,[36] M. Bhattacharjee,[44] N. Biswas,[34] G. Blazey,[32] S. Blessing,[15] P. Bloom,[7] A. Boehnlein,[14] N.I. Bojko,[37] F. Borcherding,[14] C. Boswell,[9] A. Brandt,[14] R. Brock,[27] A. Bross,[14] D. Buchholz,[33] V.S. Burtovoi,[37] J.M. Butler,[3] W. Carvalho,[10] D. Casey,[41] Z. Casilum,[44] H. Castilla-Valdez,[11] D. Chakraborty,[44] S.-M. Chang,[31] S.V. Chekulaev,[37] L.-P. Chen,[23] W. Chen,[44] S. Choi,[43] S. Chopra,[26] B.C. Choudhary,[9] J.H. Christenson,[14] M. Chung,[17] D. Claes,[29] A.R. Clark,[23] W.G. Cobau,[25] J. Cochran,[9] L. Coney,[34] W.E. Cooper,[14] C. Cretsinger,[41] D. Cullen-Vidal,[5] M.A.C. Cummings,[32] D. Cutts,[5] O.I. Dahl,[23] K. Davis,[2] K. De,[46] K. Del Signore,[26] M. Demarteau,[14] D. Denisov,[14] S.P. Denisov,[37] H.T. Diehl,[14] M. Diesburg,[14] G. Di Loreto,[27] P. Draper,[46] Y. Ducros,[42] L.V. Dudko,[28] S.R. Dugad,[45] D. Edmunds,[27] J. Ellison,[9] V.D. Elvira,[44] R. Engelmann,[44] S. Eno,[25] G. Eppley,[39] P. Ermolov,[28] O.V. Eroshin,[37] V.N. Evdokimov,[37] T. Fahland,[8] M.K. Fatyga,[41] S. Feher,[14] D. Fein,[2] T. Ferbel,[41] G. Finocchiaro,[44] H.E. Fisk,[14] Y. Fisyak,[7] E. Flattum,[14] G.E. Forden,[2] M. Fortner,[32] K.C. Frame,[27] S. Fuess,[14] E. Gallas,[46] A.N. Galyaev,[37] P. Gartung,[9] T.L. Geld,[27] R.J. Genik II,[27] K. Genser,[14] C.E. Gerber,[14] B. Gibbard,[4] S. Glenn,[7] B. Gobbi,[33] M. Goforth,[15] A. Goldschmidt,[23] B. Gómez,[1] G. Gómez,[25] P.I. Goncharov,[37] J.L. González Solís,[11] H. Gordon,[4] L.T. Goss,[47] K. Gounder,[9] A. Goussiou,[44] N. Graf,[4] P.D. Grannis,[44] D.R. Green,[14] H. Greenlee,[14] G. Grim,[7] S. Grinstein,[6] N. Grossman,[14] P. Grudberg,[23] S. Grünendahl,[14] G. Guglielmo,[35] J.A. Guida,[2] J.M. Guida,[5] A. Gupta,[45] S.N. Gurzhiev,[37] P. Gutierrez,[35] Y.E. Gutnikov,[37] N.J. Hadley,[25] H. Haggerty,[14] S. Hagopian,[15] V. Hagopian,[15] K.S. Hahn,[41] R.E. Hall,[8] P. Hanlet,[31] S. Hansen,[14] J.M. Hauptman,[19] D. Hedin,[32] A.P. Heinson,[9] U. Heintz,[14] R. Hernández-Montoya,[11] T. Heuring,[15] R. Hirosky,[15] J.D. Hobbs,[14] B. Hoeneisen,[1,*] J.S. Hoftun,[5] F. Hsieh,[26] Ting Hu,[44] Tong Hu,[18] T. Huehn,[9] A.S. Ito,[14] E. James,[2] J. Jaques,[34] S.A. Jerger,[27] R. Jesik,[18] J.Z.-Y. Jiang,[44] T. Joffe-Minor,[33] K. Johns,[2] M. Johnson,[14] A. Jonckheere,[14] M. Jones,[16] H. Jöstlein,[14] S.Y. Jun,[33] C.K. Jung,[44] S. Kahn,[4] G. Kalbfleisch,[35] J.S. Kang,[20] D. Karmanov,[28] D. Karmgard,[15] R. Kehoe,[34] M.L. Kelly,[34] C.L. Kim,[20] S.K. Kim,[43] A. Klatchko,[15] B. Klima,[14] C. Klopfenstein,[7] V.I. Klyukhin,[37] V.I. Kochetkov,[37] J.M. Kohli,[36] D. Koltick,[38] A.V. Kostritskiy,[37] J. Kotcher,[4] A.V. Kotwal,[12] J. Kourlas,[30] A.V. Kozelov,[37] E.A. Kozlovski,[37] J. Krane,[29] M.R. Krishnaswamy,[45] S. Krzywdzinski,[14] S. Kunori,[25] S. Lami,[44] R. Lander,[7] F. Landry,[27] G. Landsberg,[14] B. Lauer,[19] A. Leflat,[28] H. Li,[44] J. Li,[46] Q.Z. Li-Demarteau,[14] J.G.R. Lima,[40] D. Lincoln,[26] S.L. Linn,[15] J. Linnemann,[27] R. Lipton,[14] Y.C. Liu,[33] F. Lobkowicz,[41] S.C. Loken,[23] S. Lökös,[44] L. Lueking,[14] A.L. Lyon,[25] A.K.A. Maciel,[10] R.J. Madaras,[23] R. Madden,[15] L. Magaña-Mendoza,[11] V. Manankov,[28] S. Mani,[7] H.S. Mao,[14,†] R. Markeloff,[32] T. Marshall,[18] M.I. Martin,[14] K.M. Mauritz,[19] B. May,[33] A.A. Mayorov,[37] R. McCarthy,[44] J. McDonald,[15] T. McKibben,[17] J. McKinley,[27] T. McMahon,[35] H.L. Melanson,[14] M. Merkin,[28] K.W. Merritt,[14] H. Miettinen,[39] A. Mincer,[30] C.S. Mishra,[14] N. Mokhov,[14] N.K. Mondal,[45] H.E. Montgomery,[14] P. Mooney,[1] H. da Motta,[10] C. Murphy,[17] F. Nang,[2] M. Narain,[14] V.S. Narasimham,[45] A. Narayanan,[2] H.A. Neal,[26] J.P. Negret,[1] P. Nemethy,[30] D. Norman,[47] L. Oesch,[26] V. Oguri,[40] E. Oltman,[23] N. Oshima,[14] D. Owen,[27] P. Padley,[39] A. Para,[14] Y.M. Park,[21] R. Partridge,[5] N. Parua,[45] M. Paterno,[41] B. Pawlik,[22] J. Perkins,[46] M. Peters,[16] R. Piegaia,[6] H. Piekarz,[15] Y. Pischalnikov,[38] V.M. Podstavkov,[37] B.G. Pope,[27] H.B. Prosper,[15] S. Protopopescu,[4] J. Qian,[26] P.Z. Quintas,[14] R. Raja,[14] S. Rajagopalan,[4] O. Ramirez,[17] L. Rasmussen,[44] S. Reucroft,[31] M. Rijssenbeek,[44] T. Rockwell,[27] N.A. Roe,[23] P. Rubinov,[33] R. Ruchti,[34] J. Rutherfoord,[2] A. Sánchez-Hernández,[11] A. Santoro,[10] L. Sawyer,[24] R.D. Schamberger,[44] H. Schellman,[33] J. Sculli,[30] E. Shabalina,[28] C. Shaffer,[15] H.C. Shankar,[45] R.K. Shivpuri,[13] M. Shupe,[2] H. Singh,[9] J.B. Singh,[36] V. Sirotenko,[32] W. Smart,[14] E. Smith,[35] R.P. Smith,[14] R. Snihur,[33] G.R. Snow,[29] J. Snow,[35] S. Snyder,[4] J. Solomon,[17] P.M. Sood,[36] M. Sosebee,[46] N. Sotnikova,[28] M. Souza,[10] A.L. Spadafora,[23] G. Steinbrueck,[35] R.W. Stephens,[46] M.L. Stevenson,[23] D. Stewart,[26] F. Stichelbaut,[44] D.A. Stoianova,[37] D. Stoker,[8] M. Strauss,[35] K. Streets,[30] M. Strovink,[23] A. Sznajder,[10] P. Tamburello,[25] J. Tarazi,[8] M. Tartaglia,[14] T.L.T. Thomas,[33] J. Thompson,[25] T.G. Trippe,[23] P.M. Tuts,[12] N. Varelas,[17] E.W. Varnes,[23] D. Vititoe,[2] A.A. Volkov,[37] A.P. Vorobiev,[37] H.D. Wahl,[15] G. Wang,[15] J. Warchol,[34] G. Watts,[5] M. Wayne,[34] H. Weerts,[27] A. White,[46] J.T. White,[47] J.A. Wightman,[19] S. Willis,[32] S.J. Wimpenny,[9] J.V.D. Wirjawan,[47] J. Womersley,[14] E. Won,[41] D.R. Wood,[31] H. Xu,[5] R. Yamada,[14] P. Yamin,[4] J. Yang,[30] T. Yasuda,[31] P. Yepes,[39] C. Yoshikawa,[16] S. Youssef,[15] J. Yu,[14] Y. Yu,[43] Z.H. Zhu,[41] D. Zieminska,[18] A. Zieminski,[18] E.G. Zverev,[28] and A. Zylberstejn[42]

(DØ Collaboration)

[1] *Universidad de los Andes, Bogotá, Colombia*
[2] *University of Arizona, Tucson, Arizona 85721*
[3] *Boston University, Boston, Massachusetts 02215*
[4] *Brookhaven National Laboratory, Upton, New York 11973*
[5] *Brown University, Providence, Rhode Island 02912*
[6] *Universidad de Buenos Aires, Buenos Aires, Argentina*
[7] *University of California, Davis, California 95616*
[8] *University of California, Irvine, California 92697*
[9] *University of California, Riverside, California 92521*
[10] *LAFEX, Centro Brasileiro de Pesquisas Físicas, Rio de Janeiro, Brazil*
[11] *CINVESTAV, Mexico City, Mexico*
[12] *Columbia University, New York, New York 10027*
[13] *Delhi University, Delhi, India 110007*
[14] *Fermi National Accelerator Laboratory, Batavia, Illinois 60510*
[15] *Florida State University, Tallahassee, Florida 32306*
[16] *University of Hawaii, Honolulu, Hawaii 96822*
[17] *University of Illinois at Chicago, Chicago, Illinois 60607*
[18] *Indiana University, Bloomington, Indiana 47405*
[19] *Iowa State University, Ames, Iowa 50011*
[20] *Korea University, Seoul, Korea*
[21] *Kyungsung University, Pusan, Korea*
[22] *Institute of Nuclear Physics, Kraków, Poland*
[23] *Lawrence Berkeley National Laboratory and University of California, Berkeley, California 94720*
[24] *Louisiana Tech University, Ruston, Louisiana 71272*
[25] *University of Maryland, College Park, Maryland 20742*
[26] *University of Michigan, Ann Arbor, Michigan 48109*
[27] *Michigan State University, East Lansing, Michigan 48824*
[28] *Moscow State University, Moscow, Russia*
[29] *University of Nebraska, Lincoln, Nebraska 68588*
[30] *New York University, New York, New York 10003*
[31] *Northeastern University, Boston, Massachusetts 02115*
[32] *Northern Illinois University, DeKalb, Illinois 60115*
[33] *Northwestern University, Evanston, Illinois 60208*
[34] *University of Notre Dame, Notre Dame, Indiana 46556*
[35] *University of Oklahoma, Norman, Oklahoma 73019*
[36] *University of Panjab, Chandigarh 16-00-14, India*
[37] *Institute for High Energy Physics, 142-284 Protvino, Russia*
[38] *Purdue University, West Lafayette, Indiana 47907*
[39] *Rice University, Houston, Texas 77005*
[40] *Universidade do Estado do Rio de Janeiro, Brazil*
[41] *University of Rochester, Rochester, New York 14627*
[42] *CEA, DAPNIA/Service de Physique des Particules, CE-SACLAY, Gif-sur-Yvette, France*
[43] *Seoul National University, Seoul, Korea*
[44] *State University of New York, Stony Brook, New York 11794*
[45] *Tata Institute of Fundamental Research, Colaba, Mumbai 400005, India*
[46] *University of Texas, Arlington, Texas 76019*
[47] *Texas A&M University, College Station, Texas 77843*

A search for new physics in the channel $p\overline{p} \rightarrow \gamma\gamma jj$ has been carried out. Such a signature might characterize the production of a non- standard Higgs boson together with a W or Z. Requiring two high transverse energy photons and two jets, the diphoton mass $m_{\gamma\gamma}$ distribution is consistent with background and no resonance is observed. A 90(95)% C.L. upper limit on the cross section as a function of mass is calculated, ranging from 0.60(0.80) pb for $m_{\gamma\gamma} = 65$ GeV/c^2 to 0.26(0.34) pb for $m_{\gamma\gamma} = 150$ GeV/c^2 . For a "bosonic Higgs" having standard model couplings to vector bosons but zero coupling strength to fermions, a 95% C.L. lower mass limit is set at 81.4 GeV/c^2.

The Higgs sector of the Standard Model remains unconstrained. Several extended Higgs models [1–6] allow a light neutral scalar Higgs with suppressed couplings to fermions. The model of [1,2] gives a light neutral scalar bosonic Higgs without fine tuning and satisfies $\rho = M_W^2/M_Z^2 cos^2\theta_W = 1$, consistent with present experimental limits [7].

We shall refer to such a non-standard Higgs, having standard model strength couplings to vector bosons but zero couplings to fermions, as a "bosonic Higgs." The decay channels of this particle differ from the minimal standard model (SM) Higgs as shown in Fig. 1. Since the fermion decay channels are suppressed, the decay of the bosonic Higgs with mass less than $2m_W$ is not dominated by $H \rightarrow b\bar{b}$. At tree level the bosonic Higgs decays only to $WW^{(*)}$ and $ZZ^{(*)}$ vector bosons (where the '*' denotes that one or both of the vector bosons may be off the mass shell). For bosonic Higgs masses less than 90 GeV/c^2, the one loop, W boson mediated $H \rightarrow \gamma\gamma$ channel becomes dominant.

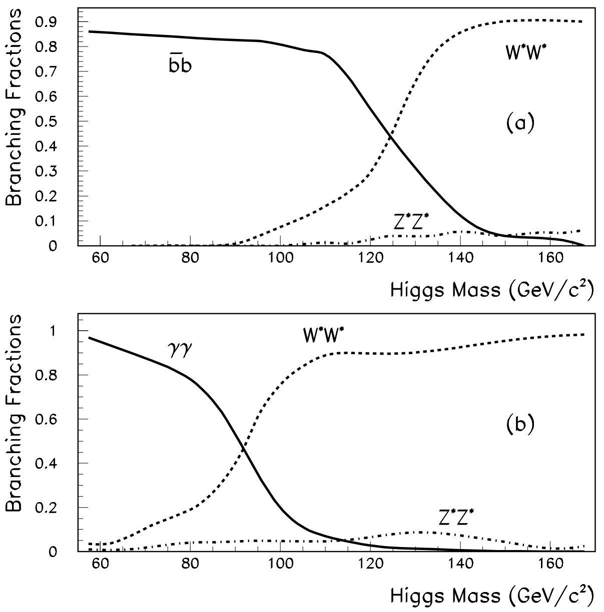

FIG. 1. Calculated branching fraction vs. Higgs mass for (a) minimal model Higgs, and (b) bosonic Higgs. In (a), the diphoton branching fraction is less than 0.001; $c\bar{c}$ and $\tau^+\tau^-$ Higgs decay channels are not shown. In (b), the Higgs decays to VV only, where VV = γ,W, or Z. Notice the large enhancement in the diphoton channel for the bosonic Higgs model: the absence of competing decay channels results in a dominant $H \rightarrow \gamma\gamma$ below $m_H \approx 90 GeV/c^2$.

A bosonic Higgs is most easily detected in the associated production mode, where an off mass shell W^* or Z^* boson is produced and radiates a Higgs boson [8]. The sum of the WH and ZH production cross sections ranges from 2 pb at m_H = 60 GeV/c^2 to 0.30 fb at m_H = 100 GeV/c^2. We expect sensitivity in the $\gamma\gamma jj$ final state up to a mass of $m_H \sim 85$ GeV/c^2 for the W and H decay modes $H \rightarrow \gamma\gamma$ and $W/Z \rightarrow jj$ The present mass limit on a bosonic Higgs is 60 GeV/c^2 from LEP1 [8,9]. Higgs production through vector boson fusion also contributes to the $\gamma\gamma jj$ final state at the 20% level, and is included in the theoretical cross section for the limit calculation.

Data corresponding to an integrated luminosity of $101.2 \pm 5.5\,\mathrm{pb}^{-1}$, recorded during 1992–96 with the DØ detector [10], are used. Photons and jets are identified using the uranium-liquid argon sampling calorimeter extending to a pseudorapidity $|\eta| = |-\ln\tan\frac{\theta}{2}| \lesssim 4$. The electromagnetic (EM) energy resolution is $\sigma_E/E = 15\%/\sqrt{E(\mathrm{GeV})} \oplus 0.3\%$, and the jet energy resolution is about $\sigma_E/E = 80\%/\sqrt{E(\mathrm{GeV})}$. The calorimeter is transversely segmented into towers in pseudorapidity and azimuthal angle of size $\Delta\eta \times \Delta\phi = 0.1 \times 0.1$, and further segmented to 0.05×0.05 at the EM shower maximum. Drift chambers in front of the calorimeter are used to distinguish photons from electrons and photon conversions. A three-level triggering system is employed: the first level used scintillation counters near the beam pipe to detect an inelastic interaction; the second level sums the EM and hadronic energy in calorimeter towers of size $\Delta\eta \times \Delta\phi = 0.2 \times 0.2$; and, the third level is a software trigger which formed clusters of calorimeter cells and applied loose cuts on the shower shape.

Events selected for this analysis had two photon candidates and two jet candidates. The first photon was required to have $E_T^\gamma > 30\,\mathrm{GeV}$, $|\eta^\gamma| < 1.1$ or $1.5 < |\eta^\gamma| < 2.0$, and the other $E_T^\gamma > 15\,\mathrm{GeV}$, $|\eta^\gamma| < 1.1$ or $1.5 < |\eta^\gamma| < 2.25$. Additionally, one hadronic jet in the event is required to have $E_T^{jet} > 30\,\mathrm{GeV}$, $|\eta^{jet}| < 2.0$, and the other hadronic jet $E_T^{jet} > 15\,\mathrm{GeV}$, $|\eta^{jet}| < 2.25$. In order for the two jets to be consistent with the decay of a W or Z boson, the dijet mass is required to be greater than 40 GeV/c^2 and less than 150 GeV/c^2. Photon candidates are rejected if there was either a reconstructed track or a significant number of drift-chamber hits in a tracking road $\Delta\theta \times \Delta\phi = 0.2 \times 0.2$ between the cluster and the vertex. A photon candidate is required to have a shape consistent with a single EM shower, to have more than 96% of its energy in the EM section of the calorimeter, and to be isolated [11]. Isolation required that the transverse energy E_T^{iso} in the annular region between $\mathcal{R} = \sqrt{\Delta\eta^2 + \Delta\phi^2} = 0.2$ and $\mathcal{R} = 0.4$ around the cluster be less than 10% of the total cluster energy, E_T^{clus}. The photon candidates are required to be well-separated from hadronic objects by requiring $\mathcal{R} > 0.7$ between every photon candidate and jet. [12]

These selections yielded four events, whose $m_{\gamma\gamma}$ distribution is shown in Fig. 2. No events are observed with $m_{\gamma\gamma} > 60\,\mathrm{GeV}$. The resolution of the detector in $m_{\gamma\gamma}$ is about 2.5 GeV/c^2 for diphoton final states passing these kinematic selections.

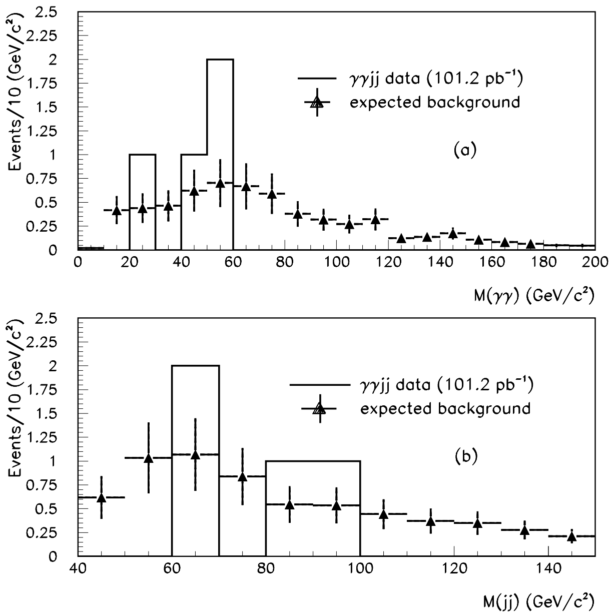

FIG. 2. The signal and expected background for (a) the diphoton mass and (b) the dijet mass distributions.

The dominant background to the $\gamma\gamma jj$ channel is QCD multijet events where two jets are misidentified as photons. During the jet fragmentation process, π^0 and η mesons are produced and will promptly decay into multiple photons. If the π^0 or η meson carries a large fraction of the jet energy and has a momentum greater than about 10 GeV/c the decay photons coalesce to mimic a single isolated photon in the calorimeter. The probability $P(j \rightarrow \text{“}\gamma\text{''})$ for a jet to mimic an isolated photon candidate in this way is estimated to be $(4.3 \pm 1.0) \times 10^{-4}$ from a fit to the longitudinal shower shape of inclusive photon candidates which determined the ratio of true photons to fluctuated jets in the sample. [12]

Smaller sources of background are true double direct photon production, single direct photon production with one jet fluctuating into a photon candidate, and final states containing electrons in addition to two jets, such as $W\gamma \rightarrow e^{\pm}\nu\gamma jj$, $Z \rightarrow e^+e^- jj$ and $t\bar{t} \rightarrow e^+e^-\nu\nu jj$ where both electron tracks fail track reconstruction and are misidentified as photons. By requiring the strict absense of a track or any significant hits in the drift chamber, the expected electron background is reduced to less than 0.01 events, and will not be considered further.

The QCD multijet background to $\gamma\gamma jj$ events is estimated from the data. Starting with the same trigger and dataset as the signal sample, a background sample is selected by requiring two EM clusters and jets, satisfying the same kinematic and fiducial cuts as the signal. Both EM clusters are required to have more than 90% of their energy in the EM section of the calorimeter, and to have no reconstructed track in the tracking road, but at least one of the two EM clusters is required to fail the photon quality criteria (isolation, shower shape, or EM fraction). The resulting sample is expected to be dominated by QCD multijet events where two jets fluctuated into highly-electromagnetic clusters. This selection yields 194 events. The distribution is normalized to the $m_{\gamma\gamma}$ sample over the bosonic Higgs excluded range $m_{\gamma\gamma} < 60 GeV/c^2$, minus the direct photon content, as an estimate of the QCD multijet background at higher $m_{\gamma\gamma}$.

The direct photon backgrounds are also calculated using the PYTHIA Monte Carlo [13]. The direct photon background has two sources, single direct photon production where one “real” photon is produced and one jet is misidentified as a photon, and double direct photon production where two “real” photons are produced, in addition to two high-E_T jets. The Monte Carlo jet and photon energies are smeared to match the measured detector resolutions. The efficiency for the events to pass the photon quality criteria (isolation, shower shape, EM fraction, and tracking) were calculated from data using our $Z \rightarrow e^+e^-$ event sample. The single direct photon events are weighted by the probability P($j \rightarrow$ “γ”), since one of the jets must be misidentified for a background event to be accepted. The direct photon background is normalized to the signal sample using the calculated direct photon cross section; the dominant systematic uncertainty in these sources of background then derives from the observed level of agreement between the theoretical and experimental direct photon cross sections, and is estimated to be 40% for double direct production and 20% for single direct photon production [11,14].

The total expected background is shown in Fig. 2 as the points with our assigned uncertainties, and it agrees well with our observed four events. We find no evidence for non-standard sources of $\gamma\gamma jj$ events. The number of QCD multijet events expected is 4.0 ± 1.5 and for direct photon events is 2.0 ± 0.6, giving a total of 6.0 ± 2.1; 4 events are observed. If we increase the γ pseudorapidity coverage to $|\eta^\gamma| < 2.5$ and reduce the leading jet and photon transverse energy requirements to 15 GeV, the same background estimation predicts 38 ± 10 events while 39 events are observed. The $m_{\gamma\gamma}$ and m_{jj} distributions of this larger sample are also well-described by the estimated background.

Simulated bosonic Higgs events are generated using PYTHIAfor the processes $p\bar{p} \rightarrow WH$ and $p\bar{p} \rightarrow ZH$, with the decays $H \rightarrow \gamma\gamma$ and $W/Z \rightarrow qq'$. Seven samples of 5000 events each are generated, having Higgs masses of 60, 70, 80, 90, 100, 110, and 150 GeV/c^2. The events are then processed through the detector simulation and the reconstruction software. The selection criteria are applied and the signal acceptance and efficiency calculated; their product ranges from 0.06 to 0.10 for Higgs masses of 60 to 150 GeV/c^2. The systematic uncertainty in the Higgs signal efficiency is based on the level of agreement between Monte Carlo and data-based estimates of the

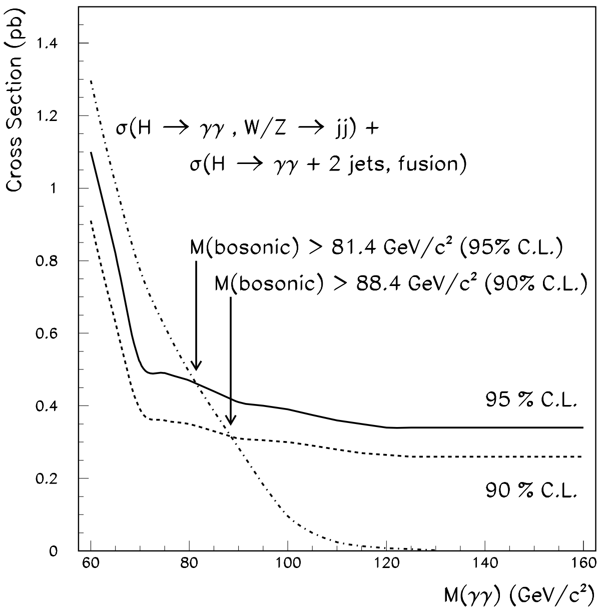

FIG. 3. The solid curve represents the 95% C.L. exclusion contour, the dashed curve represents the 90% C.L. exclusion contour, and the dot-dash curve represents the bosonic Higgs cross section with $\mathrm{H} \rightarrow \gamma\gamma$ and $\mathrm{W/Z} \rightarrow jj$ branching fractions taken into account.

photon and jet selection criteria. The systematic error includes the uncertainties from photon trigger and selection efficiences (2%), photon track requirement efficiences (12.6%), the hadronic energy scale (5-11%), the EM energy scale ($\simeq$1%), and jet reconstruction uncertainties ($\simeq$1%). The statistical uncertainty on the Monte Carlo signal samples is about 3%. The systematic and statistical uncertainties are added in quadrature and are of the order of 15%, and the luminosity uncertainty is 5.4%.

The 90% and 95% confidence level limits on the cross section as a function of $m_{\gamma\gamma}$ are shown in Fig. 3 and are calculated using a Bayesian approach [7], incorporating the errors associated with the efficiency, acceptance, luminosity, and the expected background. The full bosonic Higgs cross section is also plotted in the figure, including both the associated production and vector boson fusion production processes, calculated using PYTHIA and corrected using a K-factor of 1.25 [8]. We measure a bosonic Higgs lower mass limit of 88.4 GeV/c^2 at the 90% confidence level (CL), and lower mass limit of 81.4 GeV/c^2 at the 95% CL.

In summary, a search for new physics in the channel $p\bar{p} \rightarrow \gamma\gamma jj$ has been carried out. No candidate events are seen with a diphoton mass greater than the LEP lower mass limit of 60 GeV/c^2. Four candidates pass the selection requirements, with an expected background of 6.0 ± 2.1 events. A 90(95)% CL bosonic Higgs lower mass limit of 88.4(81.4) GeV/c^2 is set, assuming standard model coupling strengths between the Higgs and the vector bosons. A general 90(95)% C.L. upper limit on the production cross section is calculated which ranges from 0.60(0.80) *pb* for $m_{\gamma\gamma}$ = 65 GeV/c^2 to 0.26(0.34) *pb* for $m_{\gamma\gamma}$ = 150 GeV/c^2.

We thank the staffs at Fermilab and the collaborating institutions for their contributions to the success of this work, and acknowledge support from the Department of Energy and the National Science Foundation (U.S.A.), Commissariat à L'Energie Atomique (France), Ministries for Atomic Energy and Science and Technology Policy (Russia), CNPq (Brazil), Departments of Atomic Energy and Science and Education (India), Colciencias (Colombia), CONACyT (Mexico), Ministry of Education and KOSEF (Korea), CONICET and UBACyT (Argentina), and the A.P. Sloan Foundation.

---

* Visitor from IHEP, Beijing, China.

† Visitor from Univ. San Francisco de Quito, Ecuador.

[1] A.G.Akeroyd, **hep-ph/9511347**, (1995).
[2] A.G.Akeroyd, Phys. Lett. B **353**, 515 (1995).
[3] H.E. Haber, G.L. Kane, T. Sterling, Nucl. Phys. **B161**, 493 (1979).
[4] H. Pois, T. Weiler, T.C. Yuan, Phys. Rev. D **47**, 3886 (1993).
[5] P. Bamert, Z. Kunszt, Phys. Lett. B **306**, 335 (1993).
[6] H. Georgi, M. Machacek, Nucl. Phys. **B262**, 463 (1985); M. Chanowitz, M. Golden, Phys. Lett. B **165**, 105 (1985).
[7] R.M. Barnett *et. al.*, Phys. Rev. D **54**, 1 (1996).
[8] A. Stange, W. Marciano, S. Willenbrock, Phys. Rev. D **49** numb. 3 (1994).
[9] M. Acciarri *et. al.*, *Search For New Particles In Hadronic Events with Isolated Photons*, **CERN-PPE/96-50**, (1996).
[10] S. Abachi *et al.*, Nucl. Instrum. Methods **A338** (1994) 185.
[11] B. Abbott *et al.*, Phys. Rev. Lett. **78** , 2070 (1997).
[12] Bryan A. Lauer, PhD thesis, Iowa State University, Ames, IA (1997), available at http://www-d0.fnal.gov/ blauer/ thesis_100397.ps; and, D0 notes 2964, 3059 and 3176.
[13] T. Sjostrand, M. Bengtsson, Computer Physics Commun. **43** (1987) 367. Version 5.7 was used in this analysis.
[14] W. Chen, Thesis, State University of New York, Stony Brook (1997).